AN S-PALMITOYLTRANSFERASE MODULATES P2X7 FUNCTION

A Thesis

Presented to the Faculty of the Graduate School

of Cornell University

In Partial Fulfillment of the Requirements for the Degree of

Master of Science

by

Daniel Levenstein

January 2015

ABSTRACT

The P2X7 receptor is an ATP gated ion channel that plays significant roles in the immune response and neurodegeneration. In a heterologous system, P2X7 channels open only when triggered by a high concentration of ATP ($EC_{50} \approx$ 100 to 1000 μM), suggesting that P2X7 receptors may function under pathological conditions. However, it remains unclear whether P2X7 functions under physiological conditions, in which extracellular concentrations of ATP are generally much lower. Here, I show that interaction with DHHC11, a palmitoyltransferase, modifies P2X7 gating in a manner independent from its palmitoyltransferase activity. This interaction sensitizes the P2X7 receptor to lower concentrations of ATP and slows its activation and deactivation, but does not affect the so-called "dilated state" where the P2X7 channel becomes permeable to large cations. Modified P2X7 currents were still seen with deletion of the P2X7 N- and C- termini, as well as with the deletions of the DHHC11 termini. I developed a computational Markov state model and successfully replicated the observed modifications of the P2X7 receptor by DHHC11. This represents a potential interaction between P2X7 and DHHC11, which implies yet undiscovered roles of P2X7 receptor under physiological conditions.

BIOGRAPHICAL SKETCH

Dan graduated Summa Cum Laude from Northeastern University in 2011, receiving his Bachelors of Science in Biochemistry with a minor in Physics.

ACKNOWLEDGMENTS

TABLE OF CONTENTS

Introduction

ATP as a Signaling Molecule

While ATP is well known for its role as a source of energy for biological systems, it also plays an important role as an extracellular signaling molecule. The ubiquitous nature of ATP initially provided a difficult experimental hurdle in identifying the mechanism and physiological significance of many of these roles. Due to the relatively recent appreciation for its relevance (it was first proposed to be a signaling molecule by Burnstock, 1976; nearly 50 years after the discovery of ATP in 1929 (Khakh and Burnstock 2009)), purinergic signaling and its players represent a complex and under-understood system with physiological significance and therapeutic potential (Burnstock 2006).

ATP has since been found to be released in a variety of physiological situations, from apoptosis and immune activation to neuro- and gliotransmission. In the context of apoptosis/inflammation this is thought to be a "find-me" signal, alerting and directing immune cells to the location of damage (Elliott et al 2009). In the context of the central nervous system, signaling via ATP has been implicated as having a neuromodulatory role regulating functions such as long term potentiation (LTP) and neurotransmitter release (Khakh and North 2012). Extracellular ATP is thought to be released via a number of regulated pathways, most notably through large transmembrane pores such as the Pannexxin 1 channel (Chekeni et al 2010) and vesicular release from neurons and astrocytes (Pankratov et al 2007, Zhang et al 2007).

Once in the extracellular space, ATP is able to activate ionotropic P2X receptors or metabotropic P2Y receptors, and is also broken down by ectonucleotidases to ADP and then adenosine, each of which has its own cadre of membrane protein receptors (Burnstock 2007). Because ATP is able to break down and activate such a wide range of receptors, it has been challenging for the field to determine which ATP derivative/receptor combination is responsible for an elicited response in any given physiological situation. Because of these difficulties *in vivo*, our approach has been to isolate and investigate the structure/function of specific proteins using *in vitro* overexpression systems.

The P2X Receptor Ion Channel Family

Following the cloning of the seven P2X receptor subunits (P2X$_{1-7}$) (Valera et al 1994, Brake et al 1994), it was found that these proteins represent a molecularly unique family of cation-permeable ion channels and that their expression is widespread in vertebrates. The variety of functional roles ascribed to these ionotropic receptors in different tissues is astounding (Surprenant and North 2009). In the central nervous system, P2X receptors are seen in both neuronal and glial cell types (Collo et al 1997, Burnstock and Knight 2004, Rubio and Soto 2001); P2X4 and P2X6 subunits are found at postsynaptic sites in hippocampal CA1 pyramidal cells and their activation is thought to be involved in LTP by regulating the incorporation of NMDA receptors into synapses (Baxter et al 2011). In the cardiovascular system, P2X4 and P2X7 are expressed in vascular endothelial cells and P2X4 is thought to be involved in the regulation of nitric

oxide (NO) production and release (Yamamoto 2006). Most immune cells express

P2X1, P2X4, and P2X7, where their activation results in calcium influx (Burnstock and

Knight 2004) and has been shown to lead to caspase-1 activation and IL-1β (Ferrari et

al 2006). While this is not meant to be a comprehensive review, it does provide an

illustrative subset of the variety of systems for which P2X receptors play a number of

roles.

Elucidation of the molecular structure of crystalized zebrafish P2X4 (Kawate et al

2009) revealed a trimer of subunits resembling "a dolphin rising from the ocean

surface", with a large external domain that extends nearly 70 Å above the cell

membrane. Halfway up this domain resides three ATP binding sites, each located at the

interface between two subunits. Closer to the membrane, ions permeate into a central

"vestibule", which plays a role in controlling ion selectivity and from which they can

access the pore (Samways et al 2012). All P2X receptors are more permeable to Ca^{2+}

than to Na^+ ions, with P_{Ca}/P_{Na} ranging from 1.2 for P2X3 to 4.8 for P2X1 (Khakh and

North 2012). Each of the receptors display distinct functional properties and kinetic

profiles - many of the family (P2X1 and P2X3) desensitize rapidly after treatment with

ATP, and P2X2, 4, and 7 appear to undergo a phenomena termed "pore dilation",

characterized by an increase in permeability to organic cations and dyes with extended

ATP treatment (> several seconds).

P2X7 Receptors

Among the P2X family, the P2X7 receptor stands as an "odd man out". Structurally, it has a large (~200 amino acid) intracellular C-Terminal Domain (CTD) not seen in the other P2X family members (Surprenant 1996). This CTD houses potential sites for P2X7 to interact with a variety of large and small-molecule intracellular binding partners and has been implicated in regulating a number of receptor functions including downstream pathway activation and cellular localization (Costa-Junior et al 2011). Associated with the CTD is the channel's unique biphasic current profile (Fig. 1a), and the ability of the channel to "sensitize", such that ATP-induced currents of naïve (not previously exposed to ATP) receptors look drastically different than those of "sensitized"
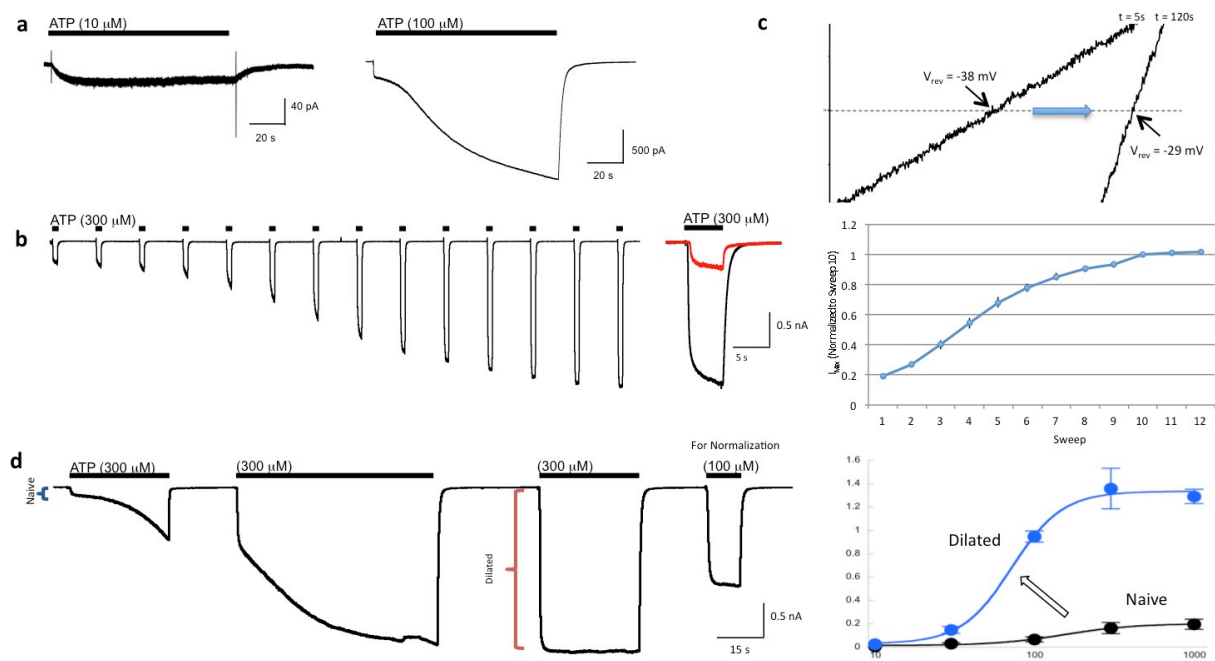

Figure 1. P2X7 currents. **a)** HEK cells transiently expressing P2X7 show small monophasic current at low (10uM, left) concentrations of ATP and biphasic current at high (100uM, right) concentrations of ATP in 0.1mM Ca-containing solution. **b)** Left: Repeated (5s every 45s) stimulation with 300uM ATP "sensitizes" P2X7 currents in transiently expressing HEK cells. Middle: 1st (red) and 10th (black) "sweep". Right: max current normalized to sweep 10 for n=7 HEK cells transfected with P2X7. **c)** Voltage ramps (-60mV to 60mV) at time t=5s and t=120s during 300uM ATP stimulation of HEK cells transfected with P2X7 in 10% Na, 90% NMDG external solution. During the course of voltage ramp protocol, V_{rev} increases from -38mV to -29mV. **d)** Left: dose response protocol for comparing the naïve and dilated P2X7. Naive P2X7-expressing HEK cells are treated with the experimental concentration of ATP (300uM shown), dilated with an 80s treatment with 300uM ATP, treated again with the experimental [ATP], and finally with 100uM ATP for normalization. Right: results of the dose response protocol for 10, 30, 100, 300, and 1000 uM ATP.

4

receptors (Fig. 1b,d). As the channel sensitizes, it becomes permeable to large cations such as NMDG. Experimentally this is evidenced by an increase in reversal potential when P2X7-expressing cells are treated with ATP in NMDG-containing external solution (Fig. 1c). Sensitized channels also show different current kinetics and ATP sensitivity than their naïve counterparts (Fig 1d). The changes associated with dilation are reversible only on the scale of hours. Additionally, P2X7 shows significantly lower affinity for ATP than the other P2X family members – with an EC_{50} in the mM range, which is way above a typical concentration of extracellular ATP under physiological circumstances.

The low affinity for ATP presents a major open question in the P2X7 field: *how does a channel that is unresponsive to physiologically relevant concentrations of ATP in vitro play a role in vivo?* While this sensitivity to high concentrations of ATP makes sense given the role of P2X7 in response to pathologically high concentrations of ATP, as seen in macrophage (Hanley et al 2012) and astrocytes (Oliveira et al 2011). It begs to question if and how this same channel is functional in more tame physiological situations, as has been shown in astrocytes (Suadicani et al 2006) and cerebellar neurons (Leon et al 2008) *in situ*, but not yet confirmed *in vivo*.

As divalent cations are allosteric inhibitors of the channel (Yan et al 2012), physiological situations associated with a drop in external calcium (such as high levels of neuronal activity) will lower the EC_{50}, but even in divalent-free solution, the channel has an EC_{50} of ~200μM ATP (naïve) (Fig 1d). Dilation increases the sensitivity of the receptor as well, with dilated channels having an EC_{50} of ~75μM in divalent-free

solution. However, a way by which receptors are able to dilate *in vivo*, which itself

requires repeated or extended stimulation by pathological concentrations of ATP, is yet

unknown. One possibility is that interactions with other cellular proteins modulate P2X7

function and sensitize the channel to lower concentrations of ATP. While these

interacting agents may be present *in vivo*, they are probably not sufficiently present in

the typical *in vitro* overexpression systems without being overexpressed themselves. In

the work reported here, I explore one proposed such possible interaction partner for

P2X7, namely palmitoylation of the protein by a palmitoyltransferase, as outlined below.

S-palmitoylation by a DHHC palmitoyltransferase represents a possible

interaction partner of P2X7

Zinc-finger, DHHC-motif containing zDHHC proteins are a family of

palmitoyltransferases. They catalyze protein S-palmitoylation, the reversible thioester

linkage of a 16-carbon palmitate lipid to an intracellular cysteine residue, via the

catalytic Asp-His-His-Cys (DHHC) region (Shipston 2011). S-palmitoylation represents a

reversable mechanism to spatiotemporally control protein function and interactions, and

has been shown to play a role in regulating the trafficking and localization of a number

of membrane proteins. The addition of palmitic acid increases the hydrophobicity of a

protein, and is thought to result in the hydrophobic tail of the palmitoyl group

"embedding" itself in the membrane, increasing a palmitoylated protein's association

with cholesterol-rich regions of the cell membrane.

While many ion channels have been shown to be palmitoylated, little is known about the effect of this modification on the gating properties of these channels. Importantly, P2X7 has been shown to be palmitoylated at a few conserved clusters of cysteine residues on the CTD (Gonnord et al 2009), however the palmitoyltransferase involved and the effect of this modification on P2X7 function is yet unknown. I propose that post-translational modification or protein-protein interactions could sensitize P2X7 to lower concentrations of ATP and that the DHHC-family of palmitoyltransferases represent good candidates for mediating this modification.

Results

Expression profiles of DHHCs and P2X7 in the Brain

While earlier work (Gonord et al 2009) suggested that P2X7 could be palmitoylated in HEK cells, it is unclear which of the 23 acyltransferaces modulate P2X7. To narrow down the DHHC proteins to a few candidates of interest, the Allen Human Brain Atlas was used to find which DHHCs are most likely to be coincident with P2X7 in vivo. Regional mRNA microarrays revealed that DHHC9, 11, and 20 are coexpressed with P2X7 (correlation of 0.883, 0.558, and 0.413, respectively) (Figure 2). Interestingly, DHHC11 and DHHC20 show alternate expression patterns in the Hypothalamus and Cerebellum, where P2X7 is highly expressed.
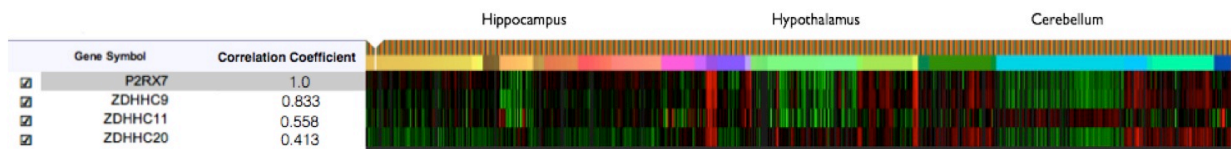

Figure 2: DHHC9, DHHC11, and DHHC20 show correlated expression with P2X7 in the human brain (Allen Brain Atlas)

DHHC11, but not DHHC9 or 20 alters P2X7 current when expressed in HEK cells

To assess the effect of DHHC proteins on P2X7 channel activity, I cotransfected P2X7 and three different DHHCs (DHHC9, 11, and 20) in HEK cells and measured ATP evoked currents (5 s applications of 300 mM ATP in 45 s intervals) using the whole-cell patch clamp configuration. This protocol allowed the measurement of kinetics of both the naïve current (the first current) and the dilated current (after repetitive ATP applications). While P2X7 currents were not visibly altered by coexpression with DHHC 9 and 20, they was dramatically altered with DHHC11 (Fig 3a).

Cotransfection with DHHC11 resulted in naïve P2X7 currents showing slower activation (Fig 3b. $\tau_{a,P2X7} = 0.33\pm0.1$s vs. $\tau_{a,P2X7+DHHC11} = 1.04\pm0.3$s) and larger max current ($I_{max,P2X7} = 755\pm103$pA vs. $I_{max,P2X7+DHHC11} = 4.34\pm0.19$nA). As previously
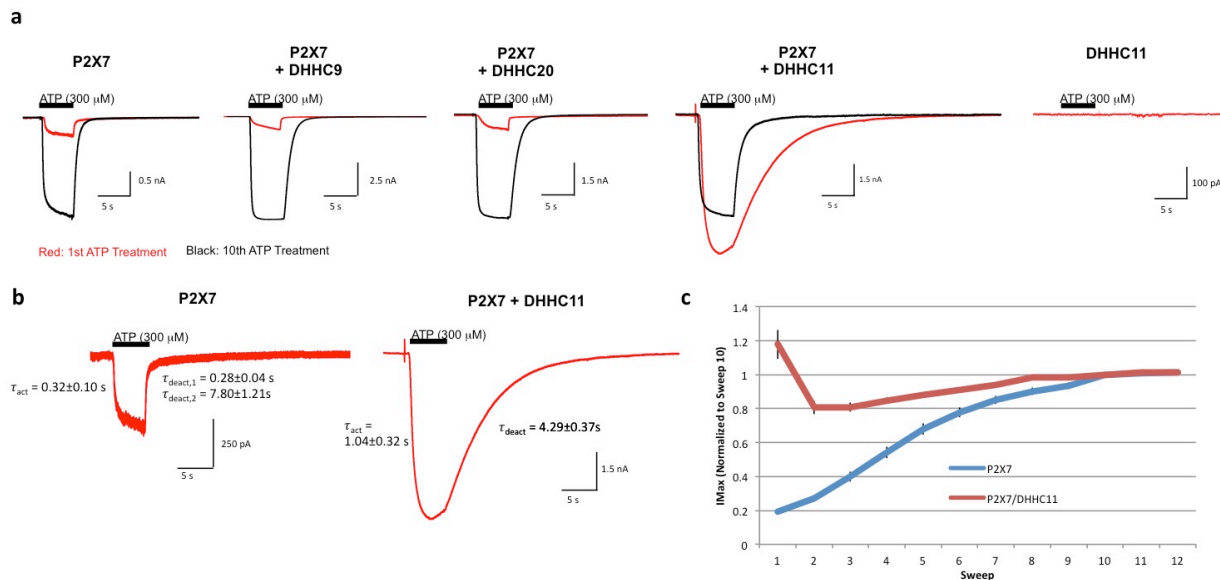

Figure 3: ATP stimulation of HEK cells coexpressing of P2X7 and DHHCs. **a)** 1st (red) and 10th (black) 300uM ATP treatment of HEK cells transfected with P2X7, P2X7 + DHHC9, P2X7 + DHHC20, P2X7 + DHHC11, and DHHC11 alone. **b)** DHHC11 alters naive P2X7 current kinetic profile, slowing down activation ($\tau_{act,\ P2X7} = 0.32\pm0.10$s, $\tau_{act,\ P2X7\ +\ DHHC11} = 1.04\pm0.32$s) and deactivation ($\tau_{deact,1,\ P2X7} = 0.28\pm0.04$ s, $\tau_{deact,2,\ P2X7} = 7.80\pm1.21$s, $\tau_{deact,\ P2X7\ +\ DHHC11} = 4.29\pm0.37$s). **c)** Max current, normalized to the 10th sweep, for 12 repeated 300uM ATP treatments of P2X7 (blue) and P2X7 + DHHC11 (red) transfected HEK cells.

8

published (Yan et al 2010), deactivation of the naïve P2X7 current fit well to a double exponential ($\tau_{d,1}$ = 7.80±1.21s and $\tau_{d,2}$ = 0.28±0.04s). However, the deactivation current for the cotransfected (P2X7 + DHHC11) condition fit much better to a single exponential (correlation coefficient: 0.96±0.01 vs. 0.78±0.06) and was much slower than the dominant term of the P2X7 alone condition ($\tau_{d,2}$) with τ_d = 4.29±0.38s (Fig 3b).

Repeated sweeps showed that the current magnitude for both conditions gradually reached a plateau, or "dilated" state (Fig 3c). Once "dilated", the ATP-induced currents of both states were indistinguishable, showing comparable activation kinetics ($\tau_{a,P2X7}$ = 0.18±0.01s; $\tau_{a,P2X7+DHHC11}$ = 0.23±0.03s), deactivation kinetics ($\tau_{d,1,P2X7}$ = 7.35±1.3s, $\tau_{d,2,P2X7}$ = 0.95±0.19s, $\tau_{d,1,P2X7+DHHC11}$ = 6.34±0.94s, $\tau_{d,2, P2X7+DHHC11}$ = 0.69±0.14s), and current magnitude ($I_{max,P2X7}$ = 3.53±0.26nA, $I_{max,P2X7+DHHC11}$ = 4.1±0.45nA). Together, these results indicate that DHHC11 affects gating of naive, but not sensitized P2X7 channels. The effect of dilation was not reversible with 30 minute wash following extended ATP treatment.

DHHC11 sensitizes the small cation-permeable P2X7 state but not the large cation-permeable state

To further characterize the current profile of the DHHC11-modulated P2X7 channel activity, co-transfected HEK cells were treated with ATP in 0.1mM Ca, 0mM Mg at a range of concentrations from 3μM to 100μM for an extended period of time (120 seconds). As seen in Figure 4a, the current show two phases at ATP concentrations of
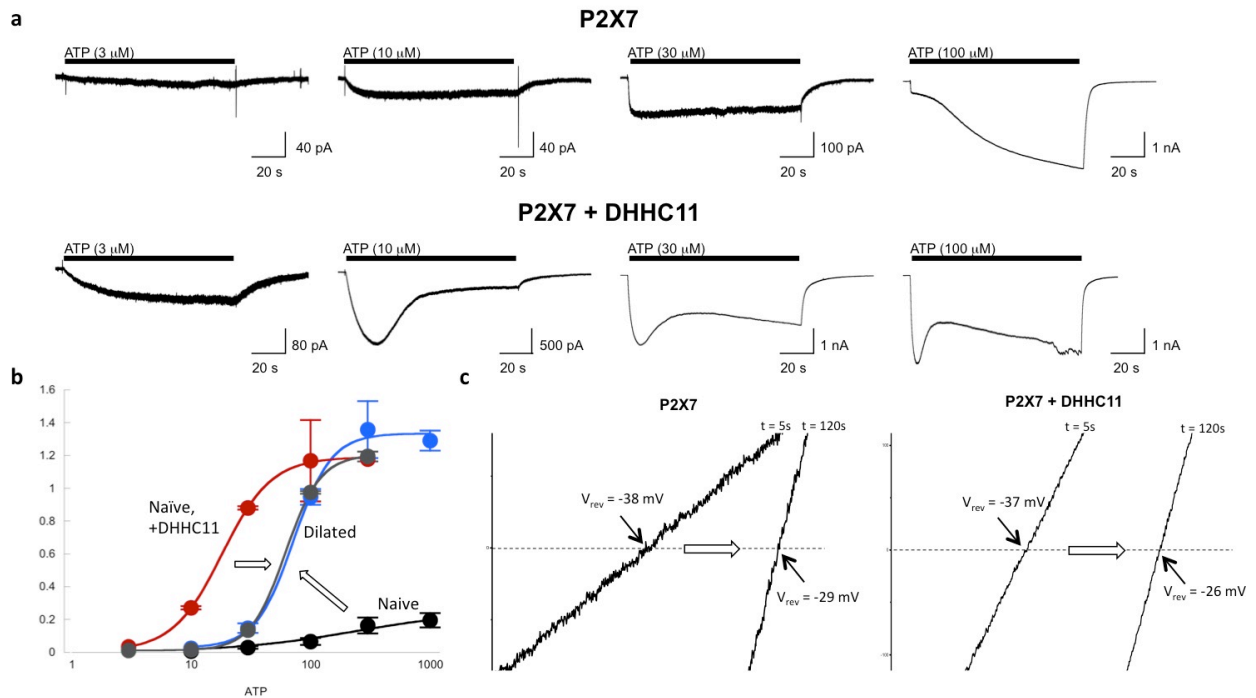
Figure 4: DHHC11 Sensitizes the P2X7 small cation current but not NMDG permeability **a)** Currents elicited by 3-100uM ATP in HEK cells transfected with P2X7 (top) and P2X7+DHHC11 (bottom). **b)** Naïve and dilated dose-response relationship for P2X7 and P2X7+DHHC11 expressing HEK cells, dose response protocol outlined in Fig 1d. **c)** Voltage ramps (-60mV to 60mV) at time t=5s and t=120s of stimulation with300uM ATP treatment of HEK cells transfected with P2X7 alone (left) and P2X7 + DHHC11 (right) in 10% Na, 90% NMDG external solution. During the course of voltage ramp protocol, V_{rev} increases from -38mV to -29mV (P2X7 alone) and 37mV to 26mV (P2X7 + DHHC11).

10μM or higher - a large initial current that desensitizes over the course of 20-50 seconds, and a slower current. While the second phase of the induced current is comparable to that seen in cells transfected with P2X7 alone, the initial current is in stark contrast to the small P2X7 initial current. Interestingly, the threshold at which a biphasic current is seen is lower than that for P2X7 alone, which shows only monophasic current with ATP consentrations lower than 100 μM. Following the dose response protocol outlined in Figure 1d, it was found that, in contrast to P2X7 alone, the naïve current of P2X7 cotransfected with DHHC11 was more sensitive to ATP than the current in the dilated state (Fig 4b).

Associated with the sensitized state is an increased permeability to large cations,

such as NMDG. To measure the change in permeability, cells were treated with ATP in

external solution with 90% of the Na^+ replaced with $NMDG^+$ and voltage was ramped

from -60 to +60mV, two times per second during ATP stimulation, following the protocol

by Yan et al 2008. As previously reported, cells expressing P2X7 are initially

impermeable to NMDG, showing a reversal potential (V_{rev}) of ~-40mV. With continued

ATP treatment, V_{rev} increases to ~-30mV, as permeability to NMDG increases. This shift

in V_{rev} was also observed in the DHHC11 cotransfected condition, indicating that the

naïve condition, while showing much larger small cation currents than those seen for

P2X7 alone, is impermeable to large cations.

DHHC11 affects P2X7 in a palmitoylation-independent manner

I then sought to assess the role of DHHC11's palmitoytransferase activity in

mediating the observed effect on P2X7 receptor ion channel function. Surprisingly,

including the reducing agent DTT in the patch pipette did not nullify the observed effect

on ATP-induced current of P2X7/DHHC11 cotransfected cells (data not shown). This

suggested 1) that the palmitoylated residue is not accessible to the cytosol and thus

was not able to be removed by DTT, 2) that palmitoylation changes the channel into a

sensitized state after which palmitoylation is not necessary, or 3) that the observed

effect is not due to DHHC11's palmitoyltransferase activity.

To test whether the effect of DHHC11 is mediated by palmitoylation, I made a

DHHC11-S mutant, with the Cys residue in the DHHC motif mutated to serine (DHHS),

as this is known to render the catalytic site nonfunctional in DHHC family members
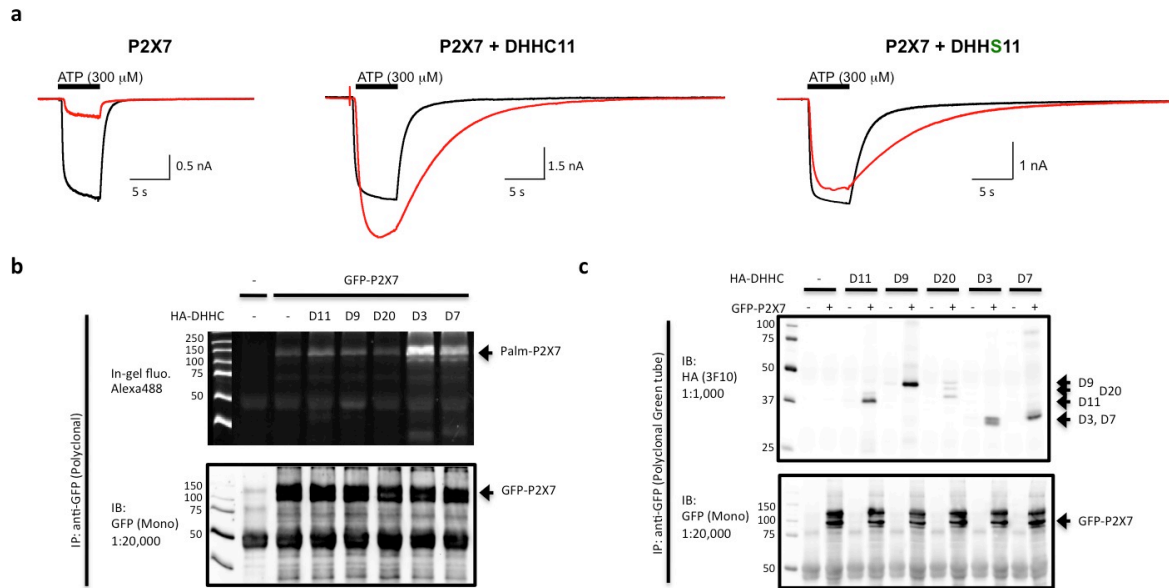
Figure 5: DHHC11 Affects P2X7 in a palmitoylation independent manner. **a)** 1st (red) and 10th (black) 300uM ATP treatment of HEK cells transfected with P2X7 (left), P2X7 + DHHC11 (middle), and P2X7 + DHHS11 (right). **b)** Palmitoylated P2X7 in HEK cells cotransfected with P2X7 and DHHC11, 9, 20, 3, 7. **c)** Co-IP of P2X7 with DHHC11, 9, 20, 3, and 7 in cotransfected HEK cells. Blots performed by Dr. Aki Nishimura.

(Maurine Linder, personal communication). Cotransfection with the DHHC11-S mutant still showed an altered P2X7 current, with slow deactivation and a large naive current (Fig 5a). Finally, Dr. Aki Nishimura performed click chemistry showing that while DHHC11 is co-immunoprecipitated with P2X7, it negligibly increases P2X7 palmitoylation above basal level (Fig 5b,c). Together these results indicate that the observed effect of DHHC11 on P2X7 function is not due that protein's palmitoyltransferase activity but is instead the result of a yet unknown interaction.

DHHC11 and P2X7 Termini are not necessary for DHHC11/P2X7 interaction

To narrow down the region of DHHC11 involved in the interaction with P2X7, I truncated the DHHC11 N- and C-Termini (DHHC11-ΔCTD: Residues 1-298. DHHC11-ΔNTD: Residues 44-348). Both of these truncations effected P2X7 currents similarly to

DHHC11-WT, (Fig 6c) indicating that the site of interaction is in one of the transmembrane helices or in the intracellular loop of DHHC11.

Similarly, I truncated the P2X7 termini (P2X7-ΔCTD: Residues 1-361. P2X7-ΔNTD: Residues 20-595). As previously reported (Becker et al 2008), deletion of the C-Terminal domain results in a P2X7 channel that only shows monophasic currents and is impermeable to NMDG, i.e. a P2X7 channel that does not dilate. I found that cotransfection with DHHC11 significantly slowed P2X7-ΔCTD current deactivation kinetics (Fig 6a,b), as seen for the wildtype P2X7 current. Unlike wildtipe P2X7, no change was seen in current magnitude with repeated ATP treatments in the presence of DHHC11. The P2X7-ΔNTD truncation also showed monophasic currents with a kinetic profile indistinguishable from the CTD truncation. This construct showed similarly
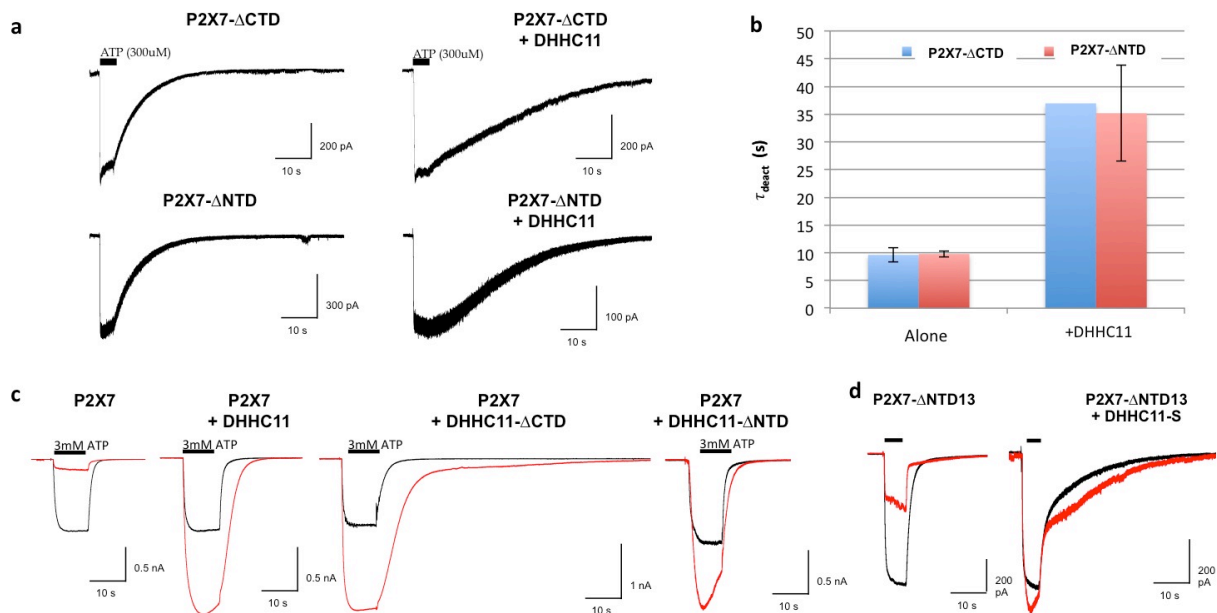

Figure 6: P2X7 and DHHC11 termini are not necessary for P2X7-DHHC11 interaction **a)** Currents elicited by 300uM ATP in HEK cells transfected with P2X7-ΔNTD (top) and P2X7-ΔCTD (top), alone (left) and with DHHC11 (right). **b)** Deactivation time constants for (a). **c)** 1st (red) and 10th (black) 300uM ATP treatment of HEK cells transfected with P2X7 alone (left), P2X7 + DHHC11 (middle-left), P2X7 + DHHC11-ΔCTD (middle-right), and , P2X7 + DHHC11-ΔNTD (right). **d)** Similar to **c** with P2X7-ΔNTD13

slowed deactivation kinetics, and again no change in the magnitude of the naïve current

(Fig 6a,b). A slightly shorter truncation of the P2X7 NTD (P2X7-ΔNTD13: Residues 13-

595) did dilate with repeated ATP treatments and when this construct was cotransfected

with DHHC11 showed both sensitization of the naïve current as well as slower

deactivation kinetics (Fig 6d). Together, these truncation results suggest that the termini

of neither protein are required for their interaction. Furthermore, they suggest that while

DHHC11 does not affect P2X7 in the dilated state, the ability of DHHC11 to potentiate

the naïve current is related to the ability of P2X7 to dilate, as this feature of the

modification is only seen in constructs for which dilation is seen

Discussion

This work identifies expression of the palmitoyltransferase DHHC11 as a factor

that alters the gating properties of the P2X7 ion channel. Cotransfection of P2X7 with

DHHC11 sensitizes naïve P2X7 to lower concentrations of ATP and slows the activation

and deactivation of the channel upon presentation and removal of ATP, respectively.

The permeability of the channel to large organic cations such as NMDG was not altered

by the presence of DHHC11, suggesting that this sensitization is distinct from the dilated

state seen with extended stimulation by ATP (Yan et al 2008). Supporting this idea,

modifications were seen to the P2X7 current in the naïve, but not the dilated state of the

channel. Neither the DHHC11 nor the P2X7 intracellular N- or C-Terminal domains were

necessary to see an effect with cotransfection with DHHC11.

Interestingly, the observed DHHC11-mediated effect on P2X7 function was shown to be independent from DHHC11's palmitoyltransferase activity, as mutating the DHHC11 palmitoyltransferase catalytic site did not rescue normal P2X7 function and cotransfection with DHHC11 did not increase P2X7 palmitoylation above basal level. I did, however, discover that two other members of the DHHC family, DHHC3 and DHHC7, do increase palmitoylation of P2X7 above basal level. Preliminary electrophysiological data suggests that palmitoylation through DHHC 3 or 7 inhibits P2X7 channel opening (data not shown), and work to characterize this effect represents an interesting direction for further research.

P2X7+DHHC11 Model

To quantitatively test potential models of how DHHC11 alters P2X7 function, I developed a "reduced" P2X7 model based on the model proposed by Yan et al 2010. The reduced model consists of five states: one naïve closed state, two naïve open states (one with high sensitivity to ATP, and one with low sensitivity to ATP and with the ability to dilate), and two dilated states, one open and one closed (Fig 7a). States and the transitions between them are described by the five linear ordinary differential equations in Table 1; the variable for each state in the model is bounded between 0 and 1 and represents the fraction of receptors in that state at a given time.

Unlike the previously proposed model, I did not take into account the number of bound ATP molecules, but focused instead on the minimal states and transitions that would be necessary to reproduce the experimentally observed P2X7 current. Namely,

15

biphasic kinetics from the naïve state are sufficiently modeled by two successive open

states, the first with higher sensitivity to ATP than the second ($k_1 > k_2$), and with the

second able to irreversibly access a higher-conductance dilated state. Once in the

dilated state, experimental results show that activation and deactivation are

monophasic, and can thus be represented by a single open and closed state. Because

dilation is irreversible on the time scale of any single experiment I did not include a

transition from the dilated to the naïve state. To further simplify the model, I

nondimensionalized agonist concentration and conductance, such that the input, A(t), is

in terms of agonist concentration relative to the EC_{50} of the dilated state and the output,

G, is in terms of conductance normalized to the maximum conductance of the dilated

state. This model is able to reproduce the fundamental features of the P2X7 current
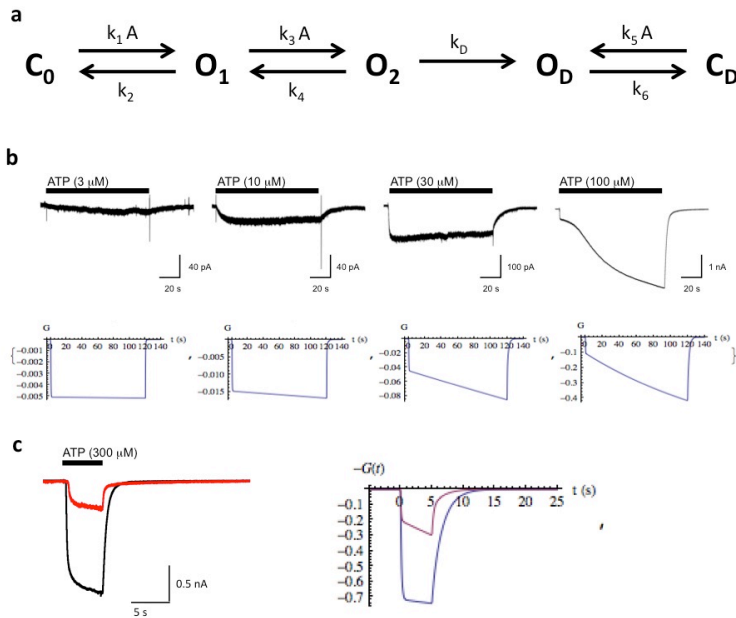
profile with minimal parameters (Fig 7 c,d).

$$\dot{C}_0 = k_2 O_1 - k_1 A C_0 \tag{1}$$
$$\dot{O}_1 = k_1 A C_0 + k_4 O_2 - (k_2 + k_3 A) O_1 \tag{2}$$
$$\dot{O}_2 = k_3 A O_1 - (k_4 + k_D) O_2 \tag{3}$$
$$\dot{O}_D = k_D O_2 + k_5 A C_D - k_6 O_D \tag{4}$$
$$\dot{C}_D = k_6 O_D - k_5 A C_D \tag{5}$$

$$G = g_{tot} / g_{dilated} = g_{12}(O_1 + O_2) + O_D \tag{6}$$

$k_1 = 0.75$ s^{-1}
$k_2 = 4.8$ s^{-1}
$k_3 = 0.053$ s^{-1}
$k_4 = 4.74$ s^{-1}
$k_D = 0.5$ s^{-1}
$k_5 = 0.6$ s^{-1}
$k_6 = 0.6$ s^{-1}

$A = [Agonist] / EC50_{Dilated}$
$g_{12} = g_{Naive} / g_{Dilated} = 0.33$

Figure 7: Reduced P2X7 model. **a)** Model diagram. **b)** Experimental (top) and simulated (bottom) P2X7 currents in response to 120s treatment with ATP (3, 10, 30, 100 um). **c)** 1st (red) and 10th (black/blue) Experimental (left) and simulated (right) P2X7 currents in response to repeated 5s treatment with ATP (300uM)

Table 1: Reduced P2X7 model equations and parameters

I propose that interaction with DHHC11 transitions the closed P2X7 receptor ion channel to a "parallel" closed state, which is able to access an alternate open state. This open state has higher macroscopic conductance than the naïve state, presumably due to a higher open probability rather than unitary conductance, as a significantly higher unitary conductance would most likely coincide with permeability to larger cations as seen in the dilated state. Based on the fitted kinetics of the DHHC11-modified P2X7 current, I presume that the kinetic constants for activation and deactivation are smaller than those for the usual naïve closed to open transition. As shown in Fig 8, this model is able to match well with the observed currents if the DHHC affected state is able to return to the P2X7 model in a transition from the DHHC11-affected open state to state
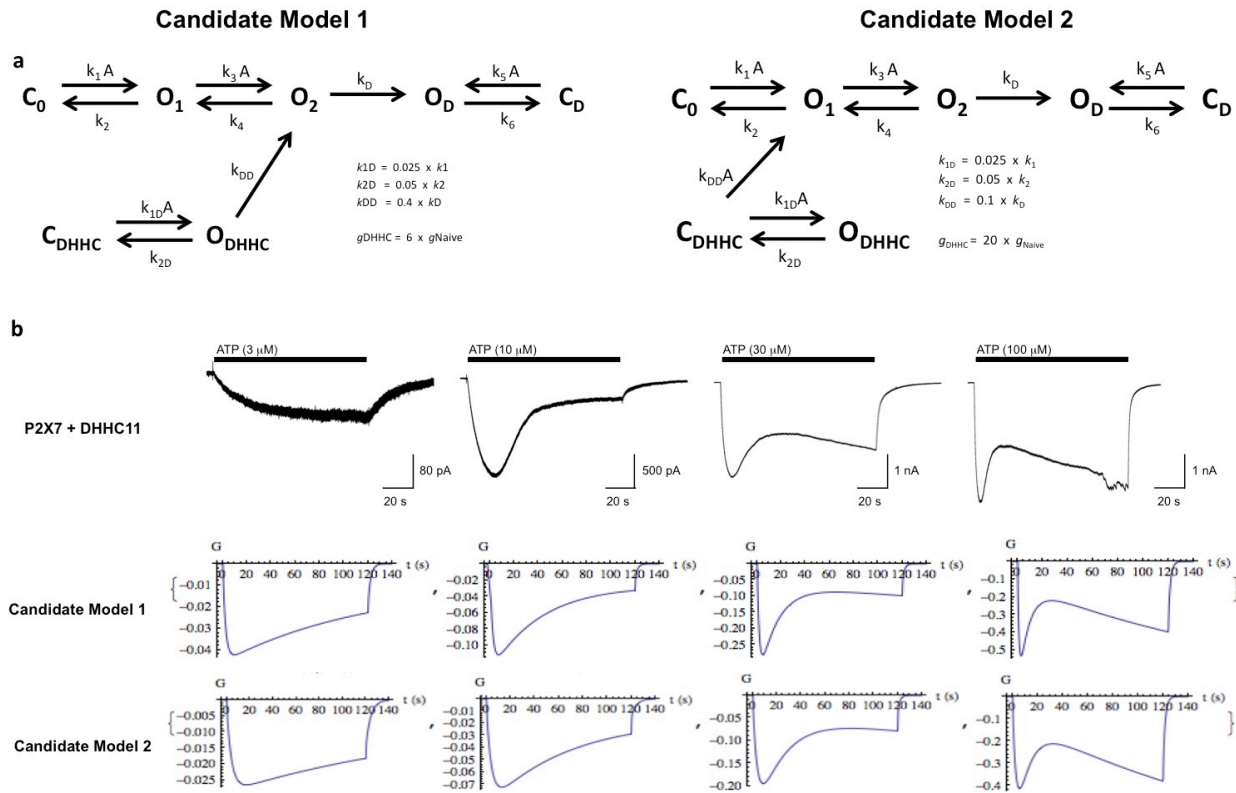

Figure 8: Candidate P2X7 + DHHC11 models **a)** Model diagram for candidate model 1 (left) and 2 (right) with added parameters. **b)** Experimental (top) and simulated currents for model 1 (middle) and 2 (bottom) in response to 120s stimulation with 3, 10, 30, and 100uM ATP.

O_2 (Candidate Model 1) or from the DHHC11-affected closed state to state O_1 (Candidate Model 2) upon treatment with ATP. Optimal fit was obtained by assuming that only a fraction of P2X7 receptors were affected by the presence of DHHC11 (50% were used for the results in Figure 8). While these were not the only model schemes that were able to fit the observed P2X7 + DHHC11 currents, they were the simplest. Experimentally testing the validity of these models is a potential area of further research for the lab.

In conclusion, the DHHC11-P2X7 interaction and its effect on P2X7 function represents a new tool for studying P2X7 function as well as a possibly physiologically significant player in the regulation of purinergic signaling. An obvious next question is "does this interaction play a role *in vivo*?" While the increase in sensitivity to extracellular ATP due to P2X7-DHHC11 interaction is a promising solution to the issue of physiological ATP concentration, further work is necessary to identify its significance. This represents a promising future direction for work in the field.

Methods

Cell Culture and Transfection

HEK 293 cells were used for the expression of P2X7 and DHHC11 constructs. Cells were maintained in DMEM containing 10% FBS and 1% Gentamycin solution. Two days prior to electryphysiological recording, cells were plated on coverslips in 35mm dishes at a density of 1×10^5 cells/dish. Transfection was conducted 24hr after plating. A transfection mixture of 155uL Opti-Mem, 500ng of each experimental DNA construct, and 6uL FUGENE was mixed by pipette, incubated at RT for 15 minutes, and added to the cells with fresh culture media. Cells were then incubated in the transfection mixture for 12-15 hours, rinsed with PBS, and again replaced with fresh culture media. Electrophysiological measurements were made within 12 hours of media replacement. All mutations were made from a rat P2X7 construct or mouse DHHC11 construct also containing GFP or mCherry for cell identification.

Electrophysiology

Prior to patching, cover slips were transferred to bath external solution at room temperature. Patch pipettes were pulled and heat-polished to a final tip resistance of 2-5 MΩ. Brightly fluorescing cells with GFP or GFP/mCherry were selected for patching. Cell attached seals of >2 GΩ were obtained and whole-cell patch-clamp mode was achieved by pipette suction. For current recording, membrane potential was held at -60mV during the perfusion protocol for ATP application. To measure changes in reversal potential, voltage was ramped from -60mV to +60mV twice per second during a

120s treatment with 300uM ATP. Patch pipettes were filled with a solution containing

147mM NaCl, 10mM EGTA, and 10mM HEPES; the pH was adjusted to 7.0 with 1M

NaOH. The external solution contained 147 mM NaCl, 2 mM KCl, 0.1 mM CaCl2, 13

mM glucose, and 10 mM HEPES; the pH was adjusted to 7.3 with 1M NaOH. ATP was

added to the external solution each recording day from a 1M ATP stock solution.

Calculations

Curve fitting of currents was performed in Clampfit 10.0 using predefined

functions of exponential standard ($f(t) = A_1 exp(-t/\tau_1) + A_2 exp(-t/\tau_2) + C$). Whenever

appropriate, the data were presented as mean ± SEM values.

Mathematical Model

Modeling was carried out using the Mathematica 8 software package from

Wolfram. For P2X7 alone I used a Markov state model consisting of 5 states (see Fig. 7

and Table 1), the variable for each of which corresponds to the fraction of receptors that

are in a given state (equations are fit to data with ATP). Corresponding to this scheme is

the system of 5 linear ordinary differential equations outlined in Table 1. To minimize the

number of parameters necessary, the total conductance was normalized to the maximal

possible conductance of the dilated state (Eq. 6), such that if all receptors were in the

open dilated state ($\mathbf{O_D}(t_i) = 1$), $\mathbf{G}(t_i) = 1$. Agonist concentration, A, was similarly

normalized to the EC_{50} of the dilated state.

To model the effect of DHHC11, two additional states and thus two equations were added to the P2X7 model

CANDIDATE MODEL 1:

$$\dot{\boldsymbol{C}}_{\mathbf{DHHC}} \;=\; k_{2D}\boldsymbol{O}_{\mathbf{DHHC}} \;-\; k_{1D}A\boldsymbol{C}_{\mathbf{DHHC}}$$

$$\dot{\boldsymbol{O}}_{\mathbf{DHHC}} \;=\; k_{1D}A\boldsymbol{C}_{\mathbf{DHHC}} \;-\; (k_{2D} + k_{DD})\boldsymbol{O}_{\mathbf{DHHC}}$$

CANDIDATE MODEL 2:

$$\dot{\boldsymbol{C}}_{\mathbf{DHHC}} \;=\; k_{2D}\boldsymbol{O}_{\mathbf{DHHC}} \;-\; (k_{1D}A + k_{DD}A)\boldsymbol{C}_{\mathbf{DHHC}}$$

$$\dot{\boldsymbol{O}}_{\mathbf{DHHC}} \;=\; k_{1D}A\boldsymbol{C}_{\mathbf{DHHC}} \;-\; k_{2D}\boldsymbol{O}_{\mathbf{DHHC}}$$

and an additional term ($k_{DD}\boldsymbol{O}_{\mathbf{DHHC}}$ or $k_{DD}A\boldsymbol{C}_{\mathbf{DHHC}}$) added to the ODE for state $\boldsymbol{O}_1$ or $\boldsymbol{C}_1$, with the relevant parameters shown in Figure 8.

References

Baxter, A W, S J Choi, J A Sim. 2011. Role of P2X4 Receptors in Synaptic Strengthening in Mouse CA1 Hippocampal Neurons. *European Journal of Neuroscience*

Brake, A J, M J Wagenbach, D Julius. 1994. New Structural Motif for Ligand-Gated Ion Channels Defined by an Ionotropic ATP Receptor. *Nature* 371(6497): 519–23.

Burnstock, G. 2006. Pathophysiology and Therapeutic Potential of Purinergic Signaling. *Pharmacological reviews*.

Burnstock, G. 2007. Physiology and Pathophysiology of Purinergic Neurotransmission. *Physiological reviews* 87(2): 659–797.

Burnstock, G, Gillian E Knight. 2004. Cellular Distribution and Functions of P2 Receptor Subtypes in Different Systems. *International review of cytology* 240: 31–304.

Chekeni, Faraaz B. 2010. Pannexin 1 Channels Mediate Find-Me'signal Release and Membrane Permeability During Apoptosis. *Nature* 467(7317): 863–67.

Collo, G. 1997. Tissue Distribution of the P2X7 Receptor. *Neuropharmacology* 36(9): 1277–83.

Costa-Junior, Helio Miranda, Flávia Sarmento Vieira, Robson Coutinho-Silva. 2011. C Terminus of the P2X7 Receptor: Treasure Hunting. *Purinergic signalling* 7(1): 7–19.

Elliott, Michael R. 2009. Nucleotides Released by Apoptotic Cells Act as a Find-Me Signal to Promote Phagocytic Clearance. *Nature* 461(7261): 282–86.

Ferrari, Davide. 2006. The P2X7 Receptor: a Key Player in IL-1 Processing and Release. *Journal of immunology (Baltimore, Md. : 1950)* 176(7): 3877–83.

Gonnord, P. 2009. Palmitoylation of the P2X7 Receptor, an ATP-Gated Channel, Controls Its Expression and Association with Lipid Rafts. *FASEB* 23(3): 795–805.

Hanley, P J. 2012. Transient P2X7 Receptor Activation Triggers Macrophage Death Independent of Toll-Like Receptors 2 and 4, Caspase-1, and Pannexin-1 Proteins. *Journal of Biological Chemistry*

Kawate, T., J. C. Michel, W. T. Birdsong, and E. Gouaux. 2009. "Crystal Structure of the ATP-Gated P2X4 Ion Channel in the Closed State." *Nature*.

Khakh, Baljit S, G Burnstock. 2009. The Double Life of ATP. *Scientific American* 301(6): 84–92.

Khakh, Baljit S, R A North. 2012. Neuromodulation by Extracellular ATP and P2X Receptors in the CNS. *Neuron* 76(1): 51–69.

León, David, Jesús Sánchez-Nogueiro, Patricia Marín-García, M Teresa Miras-Portugal. 2008. Glutamate Release and Synapsin-I Phosphorylation Induced by P2X7 Receptors Activation in Cerebellar Granule Neurons. *Neurochemistry International* 52(6): 1148–59.

Oliveira, J F. 2011. Rodent Cortical Astroglia Express in Situ Functional P2X7 Receptors Sensing Pathologically High ATP Concentrations. *Cerebral Cortex* 21(4): 806–20.

Pankratov, Yuriy, Ulyana Lalo, Alexei Verkhratsky, R Alan North. 2007. Quantal Release of ATP in

Mouse Cortex. *The Journal of General Physiology* 129(3): 257–65.

Samways, DSK, Baljit S Khakh, T M Egan. 2012. Allosteric Modulation of Ca2+ Flux in Ligand-Gated Cation Channel (P2X4) by Actions on Lateral Portals. *Journal of Biological Chemistry*.

Shipston, M J. 2011. Ion Channel Regulation by Protein Palmitoylation. *Journal of Biological Chemistry* 286(11): 8709–16.

Suadicani, Sylvia O, Celia F Brosnan, Eliana Scemes. 2006. P2X7 Receptors Mediate ATP Release and Amplification of Astrocytic Intercellular Ca2+ Signaling. *The Journal of Neuroscience* 26(5): 1378–85.

Surprenant, A, R A North. 2009. Signaling at Purinergic P2X Receptors. *Annual Review of Physiology*.

Surprenant, A., F. Rassendren, E. Kawashima, and R. A. North. 1996. "The Cytolytic P2Z Receptor for Extracellular ATP Identified as a P2X Receptor (P2X7)." *Science*.

Valera, Soledad. 1994. A New Class of Ligand-Gated Ion Channel Defined by P2X Receptor for Extracellular ATP. *, Published online: 06 October 1994; l doi:10.1038/371516a0* 371(6497): 516–19.

Yamamoto, Kimiko. 2006. Impaired Flow-Dependent Control of Vascular Tone and Remodeling in P2X4-Deficient Mice. *Nature medicine* 12(1): 133–37.

Yan, Zonghe. 2008. The P2X7 Receptor Channel Pore Dilates Under Physiological Ion Conditions. *The Journal of General Physiology* 132(5): 563–73.

Yan, Zonghe. 2010. Experimental Characterization and Mathematical Modeling of P2X7 Receptor Channel Gating. *The Journal of Neuroscience* 30(42): 14213–24.

Yan, Z., A. Khadra, A. Sherman, and S. S. Stojilkovic. 2011. "Calcium-Dependent Block of P2X7 Receptor Channel Function Is Allosteric.." *The Journal of General Physiology* 138(4):437–52.

Zhang, Zhijun. 2007. Regulated ATP Release From Astrocytes Through Lysosome Exocytosis. *Nature Cell Biology* 9(8): 945–53.